

# Is the Ewald summation still necessary? Pairwise alternatives to the accepted standard for long-range electrostatics

Christopher J. Fennell and J. Daniel Gezelter<sup>a)</sup>

*Department of Chemistry Biochemistry, University of Notre Dame, Notre Dame, Indiana 46556*

(Received 24 March 2006; accepted 27 April 2006; published online 19 June 2006)

We investigate pairwise electrostatic interaction methods and show that there are viable computationally efficient ( $\mathcal{O}(N)$ ) alternatives to the Ewald summation for typical modern molecular simulations. These methods are extended from the damped and cutoff-neutralized Coulombic sum originally proposed by Wolf *et al.* [J. Chem. Phys. **110**, 8255 (1999)]. One of these, the damped shifted force method, shows a remarkable ability to reproduce the energetic and dynamic characteristics exhibited by simulations employing lattice summation techniques. Comparisons were performed with this and other pairwise methods against the smooth particle-mesh Ewald summation to see how well they reproduce the energetics and dynamics of a variety of molecular simulations. © 2006 American Institute of Physics. [DOI: 10.1063/1.2206581]

## I. INTRODUCTION

In molecular simulations, proper accumulation of the electrostatic interactions is essential and is one of the most computationally demanding tasks. The common molecular mechanics force fields represent atomic sites with full or partial charges protected by Lennard-Jones (short-range) interactions. This means that nearly every pair interaction involves a calculation of charge-charge forces. Coupled with relatively long-ranged  $r^{-1}$  decay, the monopole interactions quickly become the most expensive part of molecular simulations. Historically, the electrostatic pair interaction would not have decayed appreciably within the typical box lengths that could be feasibly simulated. In the larger systems that are more typical of modern simulations, large cutoffs should be used to incorporate electrostatics correctly.

There have been many efforts to address the proper and practical handling of electrostatic interactions, and these have resulted in a variety of techniques.<sup>1-3</sup> These are typically classified as implicit methods (i.e., continuum dielectrics and static dipolar fields),<sup>4,5</sup> explicit methods (i.e., Ewald summations, interaction shifting, or truncation),<sup>6,7</sup> or a mixture of the two (i.e., reaction-field-type methods and fast multipole methods).<sup>8,9</sup> The explicit or mixed methods are often preferred because they physically incorporate solvent molecules in the system of interest, but these methods are sometimes difficult to utilize because of their high computational cost.<sup>1</sup> In addition to the computational cost, there have been some questions regarding possible artifacts caused by the inherent periodicity of the explicit Ewald summation.<sup>3</sup>

In this paper, we focus on a new set of pairwise methods devised by Wolf *et al.*,<sup>10</sup> which we further extend. These methods along with a few other mixed methods (i.e., reaction field) are compared with the smooth particle-mesh Ewald sum,<sup>8,11</sup> which is our reference method for handling long-range electrostatic interactions. The new methods for han-

dling electrostatics have the potential to scale linearly with increasing system size since they involve only simple modifications to the direct pairwise sum. They also lack the added periodicity of the Ewald sum, so they can be used for systems which are nonperiodic or which have one- or two-dimensional periodicity. Below, these methods are evaluated using a variety of model systems to establish their usability in molecular simulations.

## A. The Ewald sum

The complete accumulation of the electrostatic interactions in a system with periodic boundary conditions (PBCs) requires the consideration of the effect of all charges within a (cubic) simulation box as well as those in the periodic replicas,

$$V_{\text{elec}} = \frac{1}{2} \sum_{\mathbf{n}} \left[ \sum_{i=1}^N \sum_{j=1}^N \phi(\mathbf{r}_{ij} + L\mathbf{n}, \Omega_i, \Omega_j) \right], \quad (1)$$

where the sum over  $\mathbf{n}$  is a sum over all periodic box replicas with integer coordinates  $\mathbf{n} = (l, m, n)$ , and the prime indicates  $i=j$  are neglected for  $\mathbf{n}=0$ .<sup>12</sup> Within the sum,  $N$  is the number of electrostatic particles,  $\mathbf{r}_{ij}$  is  $\mathbf{r}_j - \mathbf{r}_i$ ,  $L$  is the cell length,  $\Omega_{i,j}$  are the Euler angles for  $i$  and  $j$ , and  $\phi$  is the solution to Poisson's equation ( $\phi(\mathbf{r}_{ij}) = q_i q_j / |\mathbf{r}_{ij}|^{-1}$  for charge-charge interactions). In the case of monopole electrostatics, Eq. (1) is conditionally convergent and is divergent for non-neutral systems.

The electrostatic summation problem was originally studied by Ewald for the case of an infinite crystal.<sup>6</sup> The approach he took was to convert this conditionally convergent sum into two absolutely convergent summations: a short-ranged real-space summation and a long-ranged reciprocal-space summation,

<sup>a)</sup> Author to whom correspondence should be addressed. Electronic mail: gezelter@nd.edu

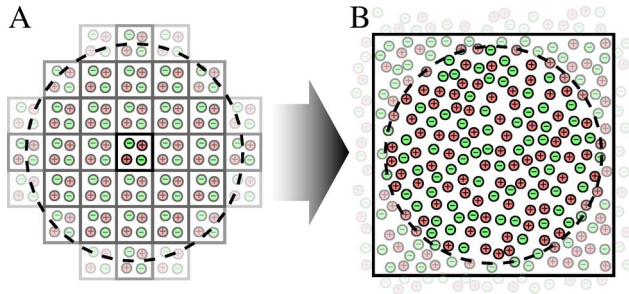


FIG. 1. The change in the need for the Ewald sum with increasing computational power. (A) Initially, only small systems could be studied, and the Ewald sum replicated the simulation box to convergence. (B) Now, radial cutoff methods should be able to reach convergence for the larger systems of charges that are common today.

$$V_{\text{elec}} = \frac{1}{2} \sum_{i=1}^N \sum_{j=1}^N \left[ q_i q_j \left( \sum_{\mathbf{n}} \frac{\text{erfc}(\alpha |\mathbf{r}_{ij} + \mathbf{n}|)}{|\mathbf{r}_{ij} + \mathbf{n}|} + \frac{1}{\pi L^3} \sum_{\mathbf{k} \neq 0} \frac{4\pi^2}{|\mathbf{k}|^2} \exp\left(-\frac{\pi^2 |\mathbf{k}|^2}{\alpha^2}\right) \cos(\mathbf{k} \cdot \mathbf{r}_{ij}) \right) \right] - \frac{\alpha}{\pi^{1/2}} \sum_{i=1}^N q_i^2 + \frac{2\pi}{(2\epsilon_s + 1)L^3} \left| \sum_{i=1}^N q_i \mathbf{r}_i \right|^2, \quad (2)$$

where  $\alpha$  is the damping or convergence parameter with units of  $\text{\AA}^{-1}$ ,  $\mathbf{k}$  are the reciprocal vectors and are equal to  $2\pi\mathbf{n}/L^2$ , and  $\epsilon_s$  is the dielectric constant of the surrounding medium. The final two terms of Eq. (2) are a particle self-term and a dipolar term for interacting with a surrounding dielectric.<sup>13</sup> This dipolar term was neglected in early applications in molecular simulations,<sup>14,15</sup> until it was introduced by de Leeuw *et al.* to address situations where the unit cell has a dipole moment which is magnified through replication of the periodic images.<sup>12,16</sup> If this term is taken to be zero, the system is said to be using conducting (or “tin-foil”) boundary conditions,  $\epsilon_s = \infty$ . Figure 1 shows how the Ewald sum has been applied over time. Initially, due to the small system sizes that could be simulated feasibly, the entire simulation box was replicated to convergence. In more modern simulations, the systems have grown large enough that a real-space cutoff could potentially give convergent behavior. Indeed, it has been observed that with the choice of a small  $\alpha$ , the reciprocal-space portion of the Ewald sum can be rapidly convergent and small relative to the real-space portion.<sup>17,18</sup>

The original Ewald summation is an  $\mathcal{O}(N^2)$  algorithm. The convergence parameter ( $\alpha$ ) plays an important role in balancing the computational cost between the direct and reciprocal-space portions of the summation. The choice of this value allows one to select whether the real-space or reciprocal space portion of the summation is an  $\mathcal{O}(N^2)$  calculation (with the other being  $\mathcal{O}(N)$ ).<sup>2</sup> With the appropriate choice of  $\alpha$  and thoughtful algorithm development, this cost can be reduced to  $\mathcal{O}(N^{3/2})$ .<sup>19</sup> The typical route taken to reduce the cost of the Ewald summation even further is to set  $\alpha$  such that the real-space interactions decay rapidly, allowing for a short spherical cutoff. Then the reciprocal space summation is optimized. These optimizations usually involve utilization of the fast Fourier transform (FFT),<sup>20</sup> leading to

the particle-particle particle-mesh (P3M) and particle-mesh Ewald (PME) methods.<sup>21–25</sup> In these methods, the cost of the reciprocal-space portion of the Ewald summation is reduced from  $\mathcal{O}(N^2)$  down to  $\mathcal{O}(N \log N)$ .

These developments and optimizations have made the use of the Ewald summation routine in simulations with periodic boundary conditions. However, in certain systems, such as vapor-liquid interfaces and membranes, the intrinsic three-dimensional periodicity can prove problematic. The Ewald sum has been reformulated to handle two-dimensional (2D) systems,<sup>26–30</sup> but these methods are computationally expensive.<sup>31,32</sup> More recently, there have been several successful efforts toward reducing the computational cost of 2D lattice summations,<sup>32–36</sup> bringing them more in line with the cost of the full three-dimensional (3D) summation.

Several studies have recognized that the inherent periodicity in the Ewald sum can also have an effect on three-dimensional systems.<sup>37–42</sup> Solvated proteins are essentially kept at high concentration due to the periodicity of the electrostatic summation method. In these systems, the more compact folded states of a protein can be artificially stabilized by the periodic replicas introduced by the Ewald summation.<sup>42</sup> Thus, care must be taken when considering the use of the Ewald summation where the assumed periodicity would introduce spurious effects in the system dynamics.

## B. The Wolf and Zahn methods

In a recent paper by Wolf *et al.*, a procedure was outlined for the accurate accumulation of electrostatic interactions in an efficient pairwise fashion. This procedure lacks the inherent periodicity of the Ewald summation.<sup>10</sup> Wolf *et al.* observed that the electrostatic interaction is effectively short ranged in condensed phase systems and that neutralization of the charge contained within the cutoff radius is crucial for potential stability. They devised a pairwise summation method that ensures charge neutrality and gives results similar to those obtained with the Ewald summation. The resulting shifted Coulomb potential includes image charges subtracted out through placement on the cutoff sphere and a distance-dependent damping function (identical to that seen in the real-space portion of the Ewald sum) to aid convergence

$$V_{\text{Wolf}}(r_{ij}) = \frac{q_i q_j \text{erfc}(\alpha r_{ij})}{r_{ij}} - \lim_{r_{ij} \rightarrow R_c} \left\{ \frac{q_i q_j \text{erfc}(\alpha r_{ij})}{r_{ij}} \right\}. \quad (3)$$

Equation (3) is essentially the common form of a shifted potential. However, neutralizing the charge contained within each cutoff sphere requires the placement of a self-image charge on the surface of the cutoff sphere. This additional self-term in the total potential enabled Wolf *et al.* to obtain excellent estimates of Madelung energies for many crystals.

In order to use their charge-neutralized potential in molecular dynamics (MD) simulations, Wolf *et al.* suggested taking the derivative of this potential prior to evaluation of the limit. This procedure gives an expression for the forces

$$F_{\text{Wolf}}(r_{ij}) = q_i q_j \left\{ \left[ \frac{\text{erfc}(\alpha r_{ij})}{r_{ij}^2} + \frac{2\alpha \exp(-\alpha^2 r_{ij}^2)}{\pi^{1/2} r_{ij}} \right] - \left[ \frac{\text{erfc}(\alpha R_c)}{R_c^2} + \frac{2\alpha \exp(-\alpha^2 R_c^2)}{\pi^{1/2} R_c} \right] \right\} \quad (4)$$

that incorporates both image charges and damping of the electrostatic interaction.

More recently, Zahn *et al.* investigated these potential and force expressions for use in simulations involving water.<sup>43</sup> In their work, they pointed out that the forces and derivative of the potential are not commensurate. Attempts to use both Eqs. (3) and (4) together will lead to poor energy conservation. They correctly observed that taking the limit shown in Eq. (3) after calculating the derivatives gives forces for a different potential energy function than the one shown in Eq. (3).

Zahn *et al.* introduced a modified form of this summation method as a way to use the technique in molecular dynamics simulations. They proposed a new damped Coulomb potential,

$$V_{\text{Zahn}}(r_{ij}) = q_i q_j \left\{ \frac{\text{erfc}(\alpha r_{ij})}{r_{ij}} - \left[ \frac{\text{erfc}(\alpha R_c)}{R_c^2} + \frac{2\alpha \exp(-\alpha^2 R_c^2)}{\pi^{1/2} R_c} \right] (r_{ij} - R_c) \right\}, \quad (5)$$

and showed that this potential does fairly well at capturing the structural and dynamic properties of water compared to the same properties obtained using the Ewald sum.

### C. Simple forms for pairwise electrostatics

The potentials proposed by Wolf *et al.* and Zahn *et al.* are constructed using two different (and separable) computational tricks: (1) shifting through the use of image charges, and (2) damping the electrostatic interaction.

Wolf *et al.* treated the development of their summation method as a progressive application of these techniques,<sup>10</sup> while Zahn *et al.* founded their damped Coulomb modification [Eq. (5)] on the postlimit forces [Eq. (4)] which were derived using both techniques. It is possible, however, to separate these tricks and study their effects independently.

Starting with the original observation that the effective range of the electrostatic interaction in condensed phases is considerably less than  $r^{-1}$ , either the cutoff sphere neutralization or the distance-dependent damping technique could be used as a foundation for a new pairwise summation method. Wolf *et al.* made the observation that charge neutralization within the cutoff sphere plays a significant role in energy convergence; therefore we will begin our analysis with the various shifted forms that maintain this charge neutralization. We can evaluate the methods of Wolf *et al.* and Zahn *et al.* by considering the standard shifted potential,

$$V_{\text{SP}}(r) = \begin{cases} v(r) - v_c, & r \leq R_c \\ 0, & r > R_c, \end{cases} \quad (6)$$

and shifted force,

$$V_{\text{SF}}(r) = \begin{cases} v(r) - v_c - \left( \frac{dv(r)}{dr} \right)_{r=R_c} (r - R_c), & r \leq R_c \\ 0, & r > R_c, \end{cases} \quad (7)$$

functions, where  $v(r)$  is the unshifted form of the potential, and  $v_c$  is  $v(R_c)$ . The shifted force (SF) form ensures that both the potential and the forces go to zero at the cutoff radius, while the shifted potential (SP) form only ensures that the potential is smooth at the cutoff radius ( $R_c$ ).<sup>13</sup>

The forces associated with the shifted potential are simply the forces of the unshifted potential itself (when inside the cutoff sphere),

$$F_{\text{SP}} = - \left( \frac{dv(r)}{dr} \right), \quad (8)$$

and are zero outside. Inside the cutoff sphere, the forces associated with the shifted force form can be written as

$$F_{\text{SF}} = - \left( \frac{dv(r)}{dr} \right) + \left( \frac{dv(r)}{dr} \right)_{r=R_c}. \quad (9)$$

If the potential,  $v(r)$ , is taken to be the normal Coulomb potential,

$$v(r) = \frac{q_i q_j}{r}, \quad (10)$$

then the SP forms will give the undamped prescription of Wolf *et al.*:

$$V_{\text{SP}}(r) = q_i q_j \left( \frac{1}{r} - \frac{1}{R_c} \right), \quad r \leq R_c, \quad (11)$$

with associated forces,

$$F_{\text{SP}}(r) = q_i q_j \left( \frac{1}{r^2} \right), \quad r \leq R_c. \quad (12)$$

These forces are identical to the forces of the standard Coulomb interaction, and cutting these off at  $R_c$  was addressed by Wolf *et al.* as undesirable. They pointed out that the effect of the image charges is neglected in the forces when this form is used,<sup>10</sup> thereby eliminating any benefit from the method in molecular dynamics. Additionally, there is a discontinuity in the forces at the cutoff radius which results in energy drift during MD simulations.

The SF form using the normal Coulomb potential will give

$$V_{\text{SF}}(r) = q_i q_j \left[ \frac{1}{r} - \frac{1}{R_c} + \left( \frac{1}{R_c^2} \right) (r - R_c) \right], \quad r \leq R_c, \quad (13)$$

with associated forces,

$$F_{\text{SF}}(r) = q_i q_j \left( \frac{1}{r^2} - \frac{1}{R_c^2} \right), \quad r \leq R_c. \quad (14)$$

This formulation has the benefit that there are no discontinuities at the cutoff radius, while the neutralizing image charges are present in both the energy and force expressions. It would be simple to add the self-neutralizing term back when computing the total energy of the system, thereby

maintaining the agreement with the Madelung energies. A side effect of this treatment is the alteration in the shape of the potential that comes from the derivative term. Thus, a degree of clarity about agreement with the empirical potential is lost in order to gain functionality in dynamics simulations.

Wolf *et al.* originally discussed the energetics of the shifted Coulomb potential [Eq. (11)] and found that it was insufficient for accurate determination of the energy with reasonable cutoff distances. The calculated Madelung energies fluctuated around the expected value as the cutoff radius was increased, but the oscillations converged toward the correct value.<sup>10</sup> A damping function was incorporated to accelerate the convergence; and though alternative forms for the damping function could be used,<sup>44,45</sup> the complimentary error function was chosen to mirror the effective screening used in the Ewald summation. Incorporating this error function damping into the simple Coulomb potential,

$$v(r) = \frac{\text{erfc}(\alpha r)}{r}, \quad (15)$$

the shifted potential [Eq. (11)] becomes

$$V_{\text{DSP}}(r) = q_i q_j \left( \frac{\text{erfc}(\alpha r)}{r} - \frac{\text{erfc}(\alpha R_c)}{R_c} \right), \quad r \leq R_c, \quad (16)$$

with associated forces,

$$F_{\text{DSP}}(r) = q_i q_j \left( \frac{\text{erfc}(\alpha r)}{r^2} + \frac{2\alpha \exp(-\alpha^2 r^2)}{\pi^{1/2} r} \right), \quad r \leq R_c. \quad (17)$$

Again, this damped shifted potential suffers from a force discontinuity at the cutoff radius, and the image charges play no role in the forces. To remedy these concerns, one may derive a SF variant by including the derivative term in Eq. (7),

$$V_{\text{DSF}}(r) = q_i q_j \left[ \frac{\text{erfc}(\alpha r)}{r} - \frac{\text{erfc}(\alpha R_c)}{R_c} + \left( \frac{\text{erfc}(\alpha R_c)}{R_c^2} + \frac{2\alpha \exp(-\alpha^2 R_c^2)}{\pi^{1/2} R_c} \right) (r - R_c) \right], \quad r \leq R_c. \quad (18)$$

The derivative of the above potential will lead to the following forces:

$$F_{\text{DSF}}(r) = q_i q_j \left[ \left( \frac{\text{erfc}(\alpha r)}{r^2} + \frac{2\alpha \exp(-\alpha^2 r^2)}{\pi^{1/2} r} \right) - \left( \frac{\text{erfc}(\alpha R_c)}{R_c^2} + \frac{2\alpha \exp(-\alpha^2 R_c^2)}{\pi^{1/2} R_c} \right) \right], \quad r \leq R_c. \quad (19)$$

If the damping parameter ( $\alpha$ ) is set to zero, the undamped case, Eqs. (11)–(14) are correctly recovered from Eqs. (16) and (19).

This new SF potential is similar to Eq. (5) derived by Zahn *et al.*; however, there are two important differences.<sup>43</sup> First, the  $v_c$  term from Eq. (7) is equal to Eq. (15) with  $r$  replaced by  $R_c$ . This term is *not* present in the Zahn potential,

resulting in a potential discontinuity as particles cross  $R_c$ . Second, the sign of the derivative portion is different. The missing  $v_c$  term would not affect molecular dynamics simulations (although the computed energy would be expected to have sudden jumps as particle distances crossed  $R_c$ ). The sign problem is a potential source of errors, however. In fact, it introduces a discontinuity in the forces at the cutoff, because the force function is shifted in the wrong direction and does not cross zero at  $R_c$ .

Equations (18) and (19) result in an electrostatic summation method in which the potential and forces are continuous at the cutoff radius and which incorporates the damping function proposed by Wolf *et al.*<sup>10</sup> In the rest of this paper, we will evaluate exactly how good these methods (SP, SF, and damping) are at reproducing the correct electrostatic summation performed by the Ewald sum.

## D. Other alternatives

In addition to the methods described above, we considered some other techniques that are commonly used in molecular simulations. The simplest of these is group-based cutoffs. Though of little use for charged molecules, collecting atoms into neutral groups takes advantage of the observation that the electrostatic interactions decay faster than those for monopolar pairs.<sup>7</sup> When considering these molecules as neutral groups, the relative orientations of the molecules control the strength of the interactions at the cutoff radius. Consequently, as these molecular particles move through  $R_c$ , the energy will drift upward due to the anisotropy of the net molecular dipole interactions.<sup>46</sup> To maintain good energy conservation, both the potential and derivative need to be smoothly switched to zero at  $R_c$ .<sup>47</sup> This is accomplished using a standard switching function. If a smooth second derivative is desired, a fifth (or higher)-order polynomial can be used.<sup>48</sup>

Group-based cutoffs neglect the surroundings beyond  $R_c$ , and to incorporate the effects of the surroundings, a method such as reaction field (RF) can be used. The original theory for RF was originally developed by Onsager,<sup>8</sup> and it was applied in simulations for the study of water by Barker and Watts.<sup>49</sup> In modern simulation codes, RF is simply an extension of the group-based cutoff method where the net dipole within the cutoff sphere polarizes an external dielectric, which reacts back on the central dipole. The same switching function considerations for group-based cutoffs need to be made for RF, with the additional prespecification of a dielectric constant.

## II. METHODS

In classical molecular mechanics simulations, there are two primary techniques utilized to obtain information about the system of interest: Monte Carlo (MC) and molecular dynamics (MD). Both of these techniques utilize pairwise summations of interactions between particle sites, but they use these summations in different ways.

In MC, the potential energy difference between configurations dictates the progression of MC sampling. Going back to the origins of this method, the acceptance criterion for the

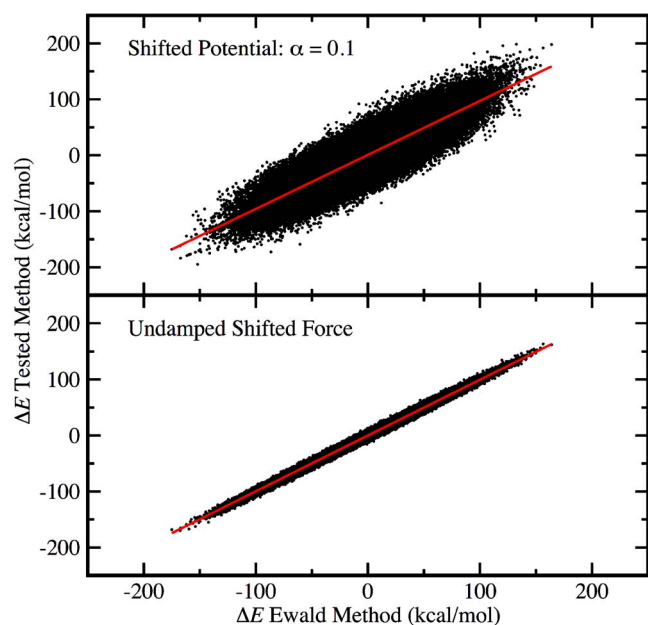


FIG. 2. Example of least squares regressions of the configuration energy differences for SPC/E water systems. The upper plot shows a data set with a poor correlation coefficient ( $R^2$ ), while the lower plot shows a data set with a good correlation coefficient.

canonical ensemble laid out by Metropolis *et al.* states that a subsequent configuration is accepted if  $\Delta E < 0$  or if  $\xi < \exp(-\Delta E/kT)$ , where  $\xi$  is a random number between 0 and 1.<sup>50</sup> Maintaining the correct  $\Delta E$  when using an alternate method for handling the long-range electrostatics will ensure proper sampling from the ensemble.

In MD, the derivative of the potential governs how the system will progress in time. Consequently, the force and torque vectors on each body in the system dictate how the system evolves. If the magnitude and direction of these vectors are similar when using alternate electrostatic summation techniques, the dynamics in the short term will be indistinguishable. Because error in MD calculations is cumulative, one should expect greater deviation at longer times, although methods which have large differences in the force and torque vectors will diverge from each other more rapidly.

### A. Monte Carlo and the energy gap

The pairwise summation techniques (outlined in Sec. II F) were evaluated for use in MC simulations by studying the energy differences between conformations. We took the smooth particle-mesh Ewald (SPME)-computed energy difference between two conformations to be the correct behavior. An ideal performance by an alternative method would reproduce these energy differences exactly (even if the absolute energies calculated by the methods are different). Since none of the methods provides exact energy differences, we used linear least squares regressions of energy gap data to evaluate how closely the methods mimicked the Ewald energy gaps. Unitary results for both the correlation (slope) and correlation coefficient for these regressions indicate perfect agreement between the alternative method and SPME. Sample correlation plots for two alternate methods are shown in Fig. 2.

Each of the seven system types (detailed in Sec. II E) was represented using 500 independent configurations. Thus, each of the alternative (non-Ewald) electrostatic summation methods was evaluated using accumulated 873 250 configurational energy differences.

Results and discussion for the individual analysis of each of the system types appear in the supporting information,<sup>51</sup> while the cumulative results over all the investigated systems appear below in Sec. III A.

### B. Molecular dynamics and the force and torque vectors

We evaluated the pairwise methods (outlined in Sec. II F) for use in MD simulations by comparing the force and torque vectors with those obtained using the reference Ewald summation (SPME). Both the magnitude and the direction of these vectors on each of the bodies in the system were analyzed. For the magnitude of these vectors, linear least squares regression analyses were performed as described previously for comparing  $\Delta E$  values. Instead of a single energy difference between two system configurations, we compared the magnitudes of the forces (and torques) on each molecule in each configuration. For a system of 1000 water molecules and 40 ions, there are 1040 force vectors and 1000 torque vectors. With 500 configurations, this results in 520 000 force and 500 000 torque vector comparisons. Additionally, data from seven different system types were aggregated before the comparison was made.

The directionality of the force and torque vectors was investigated through measurement of the angle ( $\theta$ ) formed between those computed from the particular method and those from SPME,

$$\theta_f = \cos^{-1}(\hat{F}_{\text{SPME}} \cdot \hat{F}_M), \quad (20)$$

where  $\hat{F}_M$  is the unit vector pointing along the force vector computed using method  $M$ . Each of these  $\theta$  values was accumulated in a distribution function and weighted by the area on the unit sphere. Since this distribution is a measure of angular error between two different electrostatic summation methods, there is no *a priori* reason for the profile to adhere to any specific shape. Thus, Gaussian fits were used to measure the width of the resulting distributions. The variance ( $\sigma^2$ ) was extracted from each of these fits and was used to compare distribution widths. Values of  $\sigma^2$  near zero indicate vector directions indistinguishable from those calculated when using the reference method (SPME).

### C. Short-time dynamics

The effects of the alternative electrostatic summation methods on the short-time dynamics of charged systems were evaluated by considering a NaCl crystal at a temperature of 1000 K. A subset of the best performing pairwise methods was used in this comparison. The NaCl crystal was chosen to avoid possible complications from the treatment of orientational motion in molecular systems. All systems were started with the same initial positions and velocities. Simu-

lations were performed under the microcanonical ensemble, and velocity autocorrelation functions [Eq. (21)] were computed for each of the trajectories,

$$C_v(t) = \frac{\langle v(0) \cdot v(t) \rangle}{\langle v^2 \rangle}. \quad (21)$$

Velocity autocorrelation functions require detailed short-time data, thus velocity information was saved every 2 fs over 10 ps trajectories. Because the NaCl crystal is composed of two different atom types, the average of the two resulting velocity autocorrelation functions was used for comparisons.

#### D. Long-time and collective motion

The effects of the same subset of alternative electrostatic methods on the *long-time* dynamics of charged systems were evaluated using the same model system (NaCl crystals at 1000 K). The power spectrum ( $I(\omega)$ ) was obtained via Fourier transform of the velocity autocorrelation function

$$I(\omega) = \frac{1}{2\pi} \int_{-\infty}^{\infty} C_v(t) e^{-i\omega t} dt, \quad (22)$$

where the frequency  $\omega=0, 1, \dots, N-1$ . Again, because the NaCl crystal is composed of two different atom types, the average of the two resulting power spectra was used for comparisons. Simulations were performed under the microcanonical ensemble, and velocity information was saved every 5 fs over 100 ps trajectories.

#### E. Representative simulations

A variety of representative molecular simulations was analyzed to determine the relative effectiveness of the pairwise summation techniques in reproducing the energetics and dynamics exhibited by SPME. We wanted to span the space of typical molecular simulations (i.e., from liquids of neutral molecules to ionic crystals), so the systems studied were (1) liquid water [using the extended simple point charge (SPC/E) model],<sup>52</sup> (2) crystalline water (ice  $I_c$  crystals of SPC/E), (3) NaCl crystals, (4) NaCl melts, (5) a low ionic strength solution of NaCl in water (0.11M), (6) a high ionic strength solution of NaCl in water (1.1M), and (7) a 6 Å radius sphere of argon in water.

By utilizing the pairwise techniques (outlined in Sec. II F) in systems composed entirely of neutral groups, charged particles, and mixtures of the two, we hope to discern under which conditions it will be possible to use one of the alternative summation methodologies instead of the Ewald sum.

For the solid and liquid water configurations, configurations were taken at regular intervals from high temperature trajectories of 1000 SPC/E water molecules. Each configuration was equilibrated independently at a lower temperature (300 K for the liquid, and 200 K for the crystal). The solid and liquid NaCl systems consisted of 500 Na<sup>+</sup> and 500 Cl<sup>-</sup> ions. Configurations for these systems were selected and equilibrated in the same manner as the water systems. In order to introduce measurable fluctuations in the configuration energy differences, the crystalline simulations were equilibrated at 1000 K, near the  $T_m$  for NaCl. The liquid

NaCl configurations were needed to represent a fully disordered array of point charges, so the high temperature of 7000 K was selected for equilibration. The ionic solutions were made by solvating 4 (or 40) ions in a periodic box containing 1000 SPC/E water molecules. Ion and water positions were then randomly swapped, and the resulting configurations were again equilibrated individually. Finally, for the argon/water “charge void” systems, the identities of all the SPC/E waters within 6 Å of the center of the equilibrated water configurations were converted to argon.

These procedures guaranteed us a set of representative configurations from chemically relevant systems sampled from appropriate ensembles. Force field parameters for the ions and argon were taken from the force field utilized by OOPSE.<sup>53</sup>

#### F. Comparison of summation methods

We compared the following alternative summation methods with results from the reference method (SPME): (1) SP with damping parameters ( $\alpha$ ) of 0.0, 0.1, 0.2, and 0.3 Å<sup>-1</sup>, (2) SF with damping parameters ( $\alpha$ ) of 0.0, 0.1, 0.2, and 0.3 Å<sup>-1</sup>, (3) reaction field with an infinite dielectric constant, and (4) an unmodified cutoff.

Group-based cutoffs with a fifth-order polynomial switching function were utilized for the reaction field simulations. Additionally, we investigated the use of these cutoffs with the SP, SF, and pure cutoff. The SPME electrostatics were performed using the TINKER implementation of SPME,<sup>54</sup> while all other calculations were performed using the OOPSE molecular mechanics package.<sup>53</sup> All other portions of the energy calculation (i.e. Lennard-Jones interactions) were handled in exactly the same manner across all systems and configurations.

The alternative methods were also evaluated with three different cutoff radii (9, 12, and 15 Å). As noted previously, the convergence parameter ( $\alpha$ ) plays a role in the balance of the real-space and reciprocal-space portions of the Ewald calculation. Typical molecular mechanics packages set this to a value dependent on the cutoff radius and a tolerance (typically less than  $1 \times 10^{-4}$  kcal/mol). Smaller tolerances are typically associated with increasing accuracy at the expense of computational time spent on the reciprocal-space portion of the summation.<sup>19,25</sup> The default TINKER tolerance of  $1 \times 10^{-8}$  kcal/mol was used in all SPME calculations, resulting in Ewald coefficients of 0.4200, 0.3119, and 0.2476 Å<sup>-1</sup> for cutoff radii of 9, 12, and 15 Å, respectively.

### III. RESULTS AND DISCUSSION

#### A. Configuration energy differences

In order to evaluate the performance of the pairwise electrostatic summation methods for Monte Carlo simulations, the energy differences between configurations were compared to the values obtained when using SPME. The results for the subsequent regression analysis are shown in Fig. 3.

The most striking feature of this plot is how well the SF and SP methods capture the energy differences. For the undamped SF method and the moderately damped SP methods,

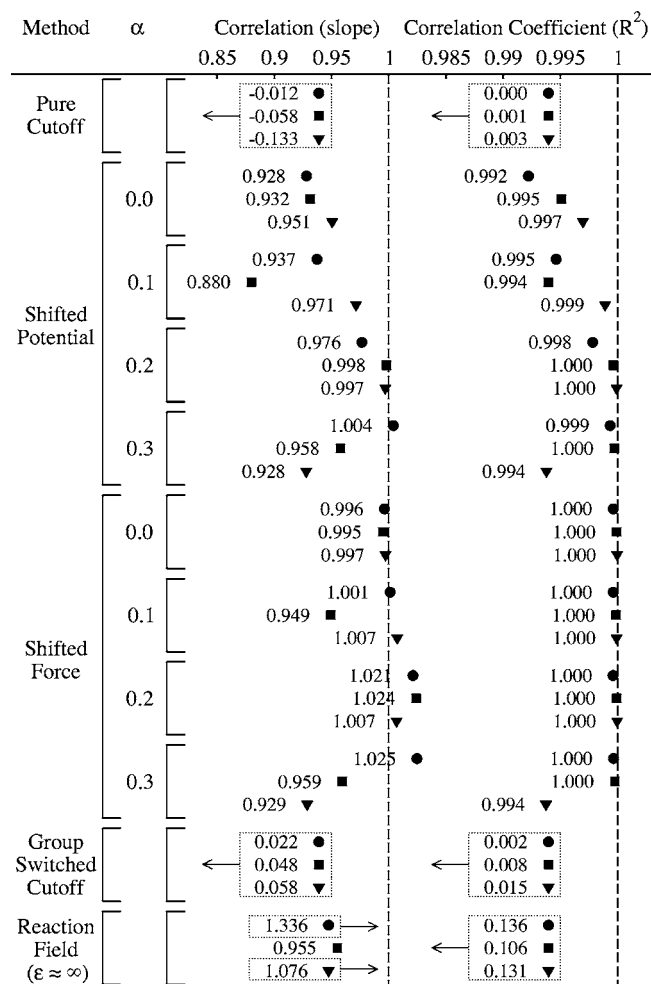


FIG. 3. Statistical analysis of the quality of configurational energy differences for a given electrostatic method compared with the reference Ewald sum. Results with a value equal to 1 (dashed line) indicate  $\Delta E$  values indistinguishable from those obtained using SPME. Different values of the cutoff radius are indicated with different symbols (9 Å=circles, 12 Å=squares, and 15 Å=inverted triangles).

the results are nearly indistinguishable from the Ewald results. The other common methods do significantly less well.

The unmodified cutoff method is essentially unusable. This is not surprising since hard cutoffs give large energy fluctuations as atoms or molecules move in and out of the cutoff radius.<sup>46,47</sup> These fluctuations can be alleviated to some degree by using group-based cutoffs with a switching function.<sup>7,47,55</sup> However, we do not see significant improvement using the group-switched cutoff because the salt and salt solution systems contain non-neutral groups. Interested readers can consult the accompanying supporting information for a comparison where all groups are neutral.<sup>51</sup>

For the SP method, inclusion of electrostatic damping improves the agreement with Ewald, and using an  $\alpha$  of 0.2 Å<sup>-1</sup> shows an excellent correlation and quality of fit with the SPME results, particularly with a cutoff radius greater than 12 Å. Use of a larger damping parameter is more helpful for the shortest cutoff shown, but it has a detrimental effect on simulations with larger cutoffs.

In the SF sets, increasing damping results in progressively *worse* correlation with Ewald. Overall, the undamped

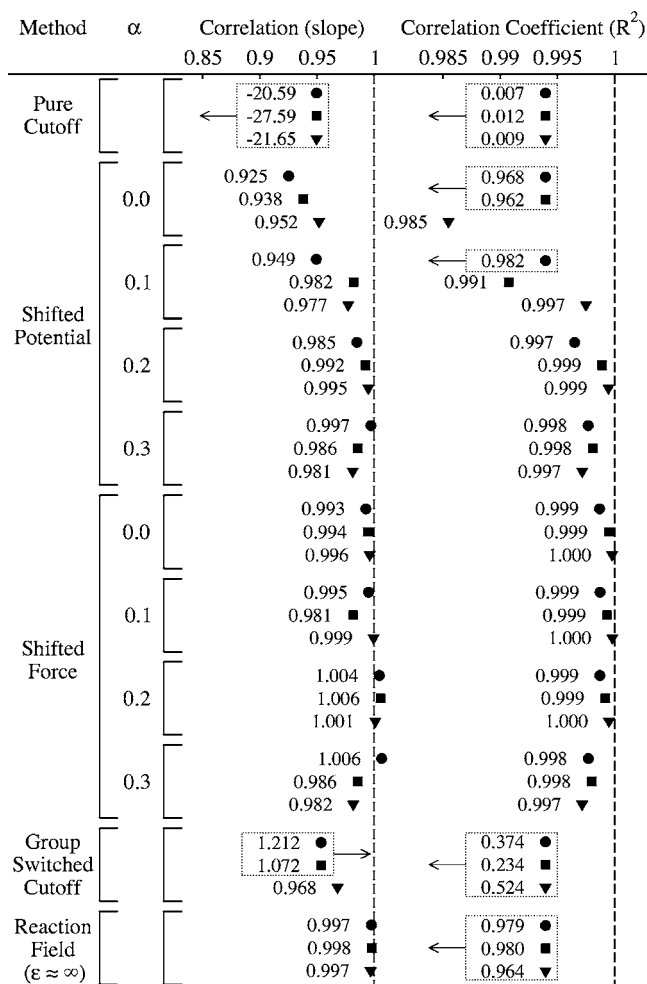


FIG. 4. Statistical analysis of the quality of the force vector magnitudes for a given electrostatic method compared with the reference Ewald sum. Results with a value equal to 1 (dashed line) indicate force magnitude values indistinguishable from those obtained using SPME. Different values of the cutoff radius are indicated with different symbols ((9 Å=circles, 12 Å=squares, and 15 Å=inverted triangles).

case is the best performing set, as the correlation and quality of fits are consistently superior regardless of the cutoff distance. The undamped case is also less computationally demanding (because no evaluation of the complementary error function is required).

The reaction field results illustrate some of that method's limitations, primarily that it was developed for use in homogenous systems, although it does provide results that are an improvement over those from an unmodified cutoff.

## B. Magnitudes of the force and torque vectors

Evaluation of pairwise methods for use in molecular dynamics simulations requires consideration of effects on the forces and torques. Figures 4 and 5 show the regression results for the force and torque vector magnitudes, respectively. The data in these figures were generated from an accumulation of the statistics from all of the system types.

Again, it is striking how well the shifted potential and shifted force methods are doing at reproducing the SPME forces. The undamped and weakly damped SF method gives the best agreement with Ewald. This is perhaps expected

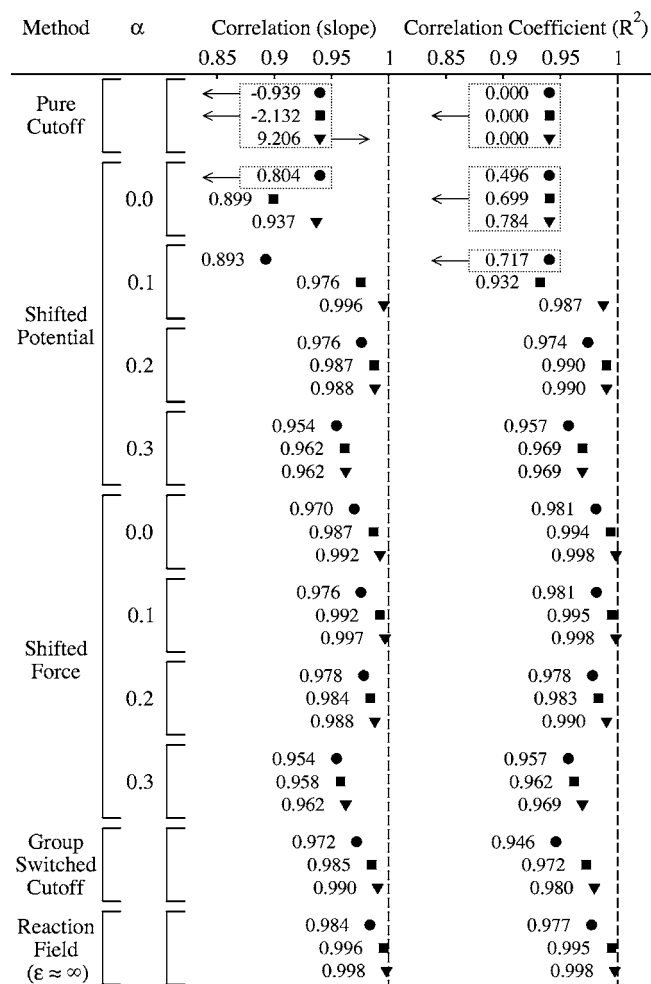


FIG. 5. Statistical analysis of the quality of the torque vector magnitudes for a given electrostatic method compared with the reference Ewald sum. Results with a value equal to 1 (dashed line) indicate torque magnitude values indistinguishable from those obtained using SPME. Different values of the cutoff radius are indicated with different symbols (9 Å=circles, 12 Å=squares, and 15 Å=inverted triangles).

because this method explicitly incorporates a smooth transition in the forces at the cutoff radius as well as the neutralizing image charges.

Figure 4, for the most part, parallels the results seen in the previous  $\Delta E$  section. The unmodified cutoff results are poor, but using group-based cutoffs and a switching function provides an improvement much more significant than what was seen with  $\Delta E$ .

With moderate damping and a large enough cutoff radius, the SP method is generating usable forces. Further increases in damping, while beneficial for simulations with a cutoff radius of 9 Å, are detrimental to simulations with larger cutoff radii.

The reaction field results are surprisingly good, considering the poor quality of the fits for the  $\Delta E$  results. There is still a considerable degree of scatter in the data, but the forces correlate well with the Ewald forces in general. We note that the reaction field calculations do not include the pure NaCl systems, so these results are partly biased towards conditions in which the method performs more favorably.

Molecular torques were only available from the systems

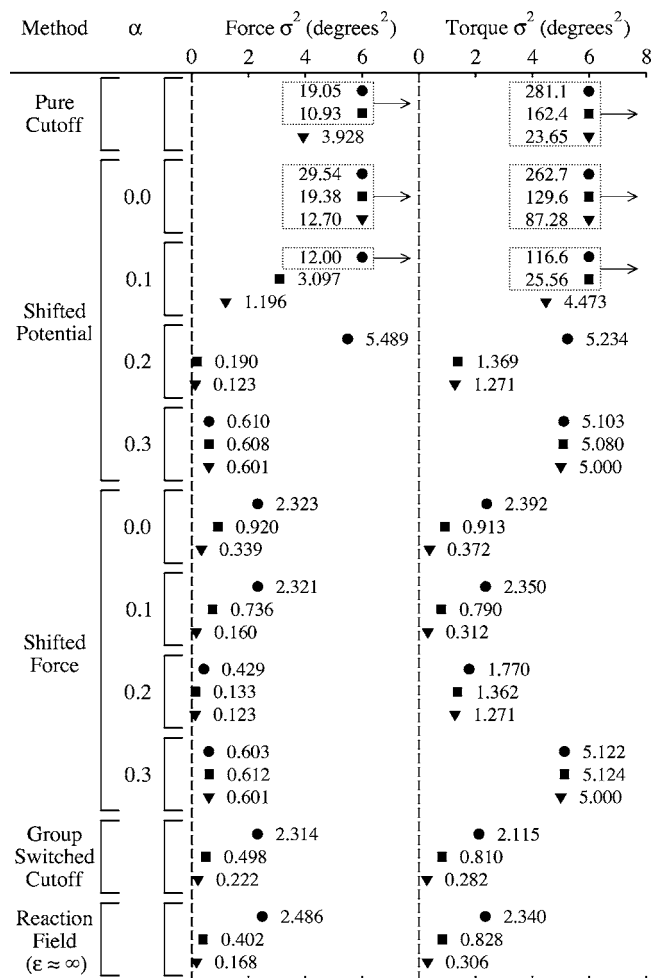


FIG. 6. Statistical analysis of the width of the angular distribution that the force and torque vectors from a given electrostatic method make with their counterparts obtained using the reference Ewald sum. Results with a variance ( $\sigma^2$ ) equal to zero (dashed line) indicate force and torque directions indistinguishable from those obtained using SPME. Different values of the cutoff radius are indicated with different symbols (9 Å=circles, 12 Å=squares, and 15 Å=inverted triangles).

which contained rigid molecules (i.e., the systems containing water). The data in Fig. 5 are taken from this smaller sampling pool.

Torques appear to be much more sensitive to charges at a longer distance. The striking feature in comparing the new electrostatic methods with SPME is how much the agreement improves with increasing cutoff radius. Again, the weakly damped and undamped SF method appears to be reproducing the SPME torques most accurately.

Water molecules are dipolar, and the reaction field method reproduces the effect of the surrounding polarized medium on each of the molecular bodies. Therefore it is not surprising that reaction field performs best of all of the methods on molecular torques.

### C. Directionality of the force and torque vectors

It is clearly important that a new electrostatic method can reproduce the magnitudes of the force and torque vectors obtained via the Ewald sum. However, the directionality of these vectors will also be vital in calculating dynamical

quantities accurately. Force and torque directionalities were investigated by measuring the angles formed between these vectors and the same vectors calculated using SPME. The results (Fig. 6) are compared through the variance ( $\sigma^2$ ) of the Gaussian fits of the angle error distributions of the combined set over all system types.

Both the force and torque  $\sigma^2$  results from the analysis of the total accumulated system data are tabulated in Fig. 6. Here it is clear that the SP method would be essentially unusable for molecular dynamics unless the damping function is added. The SF method, however, is generating force and torque vectors which are within a few degrees of the Ewald results even with weak (or no) damping.

All of the sets (aside from the overdamped case) show the improvement afforded by choosing a larger cutoff radius. Increasing the cutoff from 9 to 12 Å typically results in a halving of the width of the distribution, with a similar improvement when going from 12 to 15 Å.

The undamped SF, group-based cutoff, and reaction field methods all do equivalently well at capturing the direction of both the force and torque vectors. Using the electrostatic damping improves the angular behavior significantly for the SP and moderately for the SF methods. Overdamping is detrimental to both methods. Again it is important to recognize that the force vectors cover all particles in all seven systems, while torque vectors are only available for neutral molecular groups. Damping is more beneficial to charged bodies, and this observation is investigated further in the accompanying supporting information.<sup>51</sup>

Although not discussed previously, group based cutoffs can be applied to both the SP and SF methods. The group-based cutoffs will reintroduce small discontinuities at the cutoff radius, but the effects of these can be minimized by utilizing a switching function. Though there are no significant benefits or drawbacks observed in  $\Delta E$  and the force and torque magnitudes when doing this, there is a measurable improvement in the directionality of the forces and torques. Table I shows the angular variances obtained using group-based cutoffs along with the results seen in Fig. 6. The SP

(with an  $\alpha$  of 0.2 Å<sup>-1</sup> or smaller) shows much narrower angular distributions when using group-based cutoffs. The SF method likewise shows improvement in the undamped and lightly damped cases.

One additional trend in Table I is that the  $\sigma^2$  values for both SP and SF converge as  $\alpha$  increases, something that is more obvious with group-based cutoffs. The complimentary error function inserted into the potential weakens the electrostatic interaction as the value of  $\alpha$  is increased. However, at larger values of  $\alpha$ , it is possible to overdamp the electrostatic interaction and to remove it completely. Kast *et al.* developed a method for choosing appropriate  $\alpha$  values for these types of electrostatic summation methods by fitting to  $g(r)$  data, and their methods indicate optimal values of 0.34, 0.25, and 0.16 Å<sup>-1</sup> for cutoff values of 9, 12, and 15 Å, respectively.<sup>56</sup> These appear to be reasonable choices to obtain proper MC behavior (Fig. 3); however, based on these findings, choices this high would introduce error in the molecular torques, particularly for the shorter cutoffs. Based on our observations, empirical damping up to 0.2 Å<sup>-1</sup> is beneficial, but damping may be unnecessary when using the SF method.

#### D. Short-time dynamics: Velocity autocorrelation functions of NaCl crystals

Zahn *et al.* investigated the structure and dynamics of water using Eqs. (5) and (4).<sup>43,56</sup> Their results indicated that a method similar to (but not identical with) the damped SF method resulted in properties very similar to those obtained when using the Ewald summation. The properties they studied (pair distribution functions, diffusion constants, and velocity and orientational correlation functions) may not be particularly sensitive to the long-range and collective behavior that governs the low-frequency behavior in crystalline systems. Additionally, the ionic crystals are the worst case scenario for the pairwise methods because these methods lack the reciprocal-space contribution contained in the Ewald summation.

TABLE I. Statistical analysis of the angular distributions that the force (upper) and torque (lower) vectors from a given electrostatic method make with their counterparts obtained using the reference Ewald sum. Calculations were performed both with (Y) and without (N) group-based cutoffs and a switching function. The  $\alpha$  values have units of Å<sup>-1</sup> and the variance values have units of degrees squared.

$R_c$ (Å)	Groups	Shifted potential				Shifted force			
		$\alpha=0$	$\alpha=0.1$	$\alpha=0.2$	$\alpha=0.3$	$\alpha=0$	$\alpha=0.1$	$\alpha=0.2$	$\alpha=0.3$
9	N	29.545	12.003	5.489	0.610	2.323	2.321	0.429	0.603
	Y	2.486	2.160	0.667	0.608	1.768	1.766	0.676	0.609
12	N	19.381	3.097	0.190	0.608	0.920	0.736	0.133	0.612
	Y	0.515	0.288	0.127	0.586	0.308	0.249	0.127	0.586
15	N	12.700	1.196	0.123	0.601	0.339	0.160	0.123	0.601
	Y	0.228	0.099	0.121	0.598	0.144	0.090	0.121	0.598
9	N	262.716	116.585	5.234	5.103	2.392	2.350	1.770	5.122
	Y	2.115	1.914	1.878	5.142	2.076	2.039	1.972	5.146
12	N	129.576	25.560	1.369	5.080	0.913	0.790	1.362	5.124
	Y	0.810	0.685	1.352	5.082	0.765	0.714	1.360	5.082
15	N	87.275	4.473	1.271	5.000	0.372	0.312	1.271	5.000
	Y	0.282	0.294	1.272	4.999	0.324	0.318	1.272	4.999

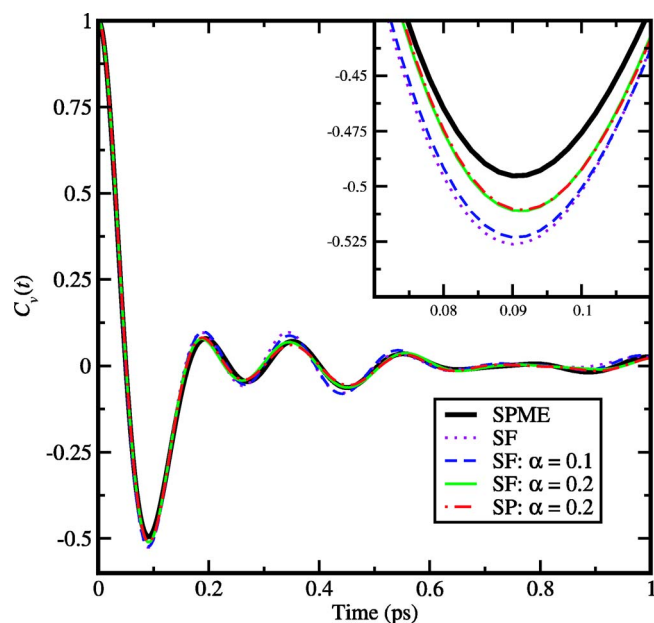


FIG. 7. Velocity autocorrelation functions of NaCl crystals at 1000 K using SPME, SF ( $\alpha=0.0, 0.1$ , and  $0.2$ ), and SP ( $\alpha=0.2$ ). The inset is a magnification of the area around the first minimum. The times to first collision are nearly identical, but differences can be seen in the peaks and troughs, where the undamped and weakly damped methods are stiffer than the moderately damped and SPME methods.

We are using two separate measures to probe the effects of these alternative electrostatic methods on the dynamics in crystalline materials. For short- and intermediate-time dynamics, we are computing the velocity autocorrelation function, and for long-time and large length-scale collective motions, we are looking at the low-frequency portion of the power spectrum.

The short-time decay of the velocity autocorrelation function through the first collision is nearly identical in Fig. 7, but the peaks and troughs of the functions show how the methods differ. The undamped SF method has deeper troughs (see inset of Fig. 7) and higher peaks than any of the other methods. As the damping parameter ( $\alpha$ ) is increased, these peaks are smoothed out, and the SF method approaches the SPME results. With  $\alpha$  values of  $0.2 \text{ \AA}^{-1}$ , the SF and SP functions are nearly identical and track the SPME features quite well. This is not surprising because the SF and SP potentials become nearly identical with increased damping. However, this appears to indicate that once damping is utilized, the details of the form of the potential (and forces) constructed out of the damped electrostatic interaction are less important.

### E. Collective motion: Power spectra of NaCl crystals

To evaluate how the differences between the methods affect the collective long-time motion, we computed power spectra from long-time traces of the velocity autocorrelation function. The power spectra for the best performing alternative methods are shown in Fig. 8. Apodization of the correlation functions via a cubic switching function between 40

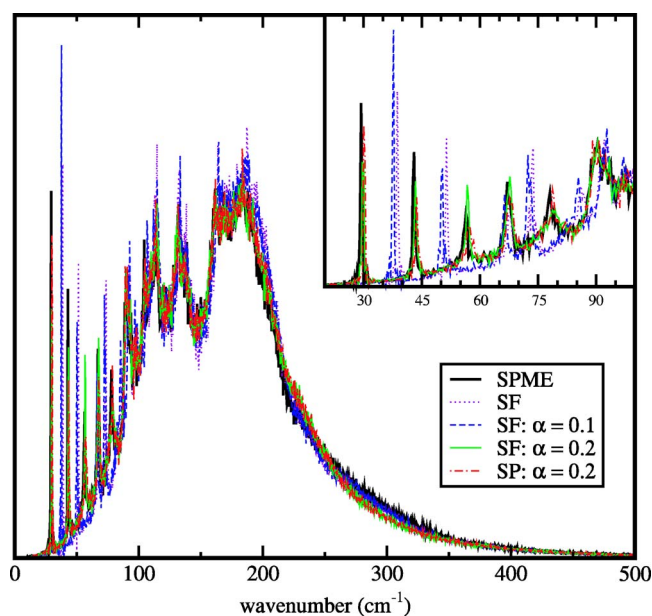


FIG. 8. Power spectra obtained from the velocity autocorrelation functions of NaCl crystals at 1000 K while using SPME, SF ( $\alpha=0, 0.1$ , and  $0.2$ ), and SP ( $\alpha=0.2$ ). The inset shows the frequency region below  $100 \text{ cm}^{-1}$  to highlight where the spectra differ.

and  $50 \text{ ps}$  was used to reduce the ringing resulting from data truncation. This procedure had no noticeable effect on peak location or magnitude.

While the high-frequency regions of the power spectra for the alternative methods are quantitatively identical with Ewald spectrum, the low-frequency region shows how the summation methods differ. Considering the low-frequency inset (expanded in the upper frame of Fig. 9), at frequencies below  $100 \text{ cm}^{-1}$ , the correlated motions are blueshifted when

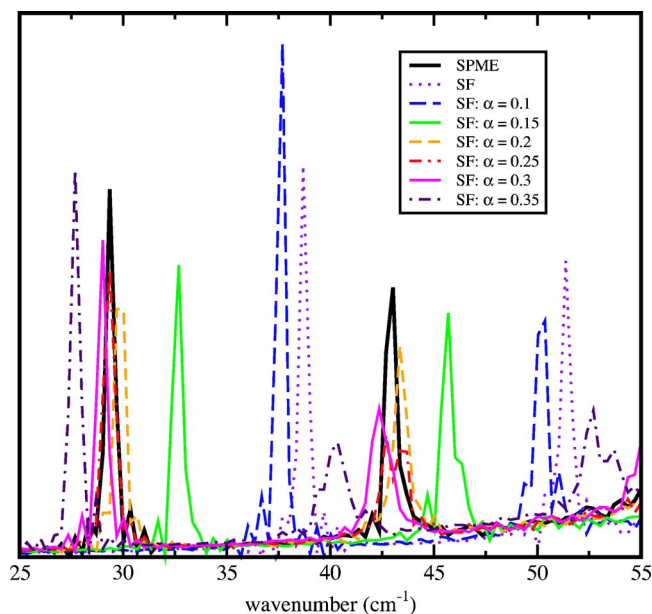


FIG. 9. Effect of damping on the two lowest-frequency phonon modes in the NaCl crystal at 1000 K. The undamped shifted force (SF) method is off by less than  $10 \text{ cm}^{-1}$ , and increasing the electrostatic damping to  $0.25 \text{ \AA}^{-1}$  gives quantitative agreement with the power spectrum obtained using the Ewald sum. Overdamping can result in underestimates of frequencies of the long-wavelength motions.

using undamped or weakly damped SF. When using moderate damping ( $\alpha=0.2 \text{ \AA}^{-1}$ ) both the SF and SP methods give nearly identical correlated motion to the Ewald method (which has a convergence parameter of  $0.3119 \text{ \AA}^{-1}$ ). This weakening of the electrostatic interaction with increased damping explains why the long-ranged correlated motions are at lower frequencies for the moderately damped methods than for undamped or weakly damped methods.

To isolate the role of the damping constant, we have computed the spectra for a single method (SF) with a range of damping constants and compared this with the SPME spectrum. Figure 9 shows more clearly that increasing the electrostatic damping redshifts the lowest-frequency phonon modes. However, even without any electrostatic damping, the SF method has at most a  $10 \text{ cm}^{-1}$  error in the lowest-frequency phonon mode. Without the SF modifications, an undamped (pure cutoff) method would predict the lowest-frequency peak near  $325 \text{ cm}^{-1}$ . Most of the collective behavior in the crystal is accurately captured using the SF method. Quantitative agreement with Ewald can be obtained using moderate damping in addition to the shifting at the cutoff distance.

#### IV. CONCLUSIONS

This investigation of pairwise electrostatic summation techniques shows that there are viable and computationally efficient alternatives to the Ewald summation. These methods are derived from the damped and cutoff-neutralized Coulombic sum originally proposed by Wolf *et al.*<sup>10</sup> In particular, the SF method, reformulated above as Eqs. (18) and (19), shows a remarkable ability to reproduce the energetic and dynamic characteristics exhibited by simulations employing lattice summation techniques. The cumulative energy difference results showed that the undamped SF and moderately damped SP methods produced results nearly identical to SPME. Similarly for the dynamic features, the undamped or moderately damped SF and moderately damped SP methods produce force and torque vector magnitude and directions very similar to the expected values. These results translate into long-time dynamic behavior equivalent to that produced in simulations using SPME.

As in all purely pairwise cutoff methods, these methods are expected to scale approximately linearly with system size, and they are easily parallelizable. This should result in substantial reductions in the computational cost of performing large simulations.

Aside from the computational cost benefit, these techniques have applicability in situations where the use of the Ewald sum can prove problematic. Of greatest interest is their potential use in interfacial systems, where the unmodified lattice sum techniques artificially accentuate the periodicity of the system in an undesirable manner. There have been alterations to the standard Ewald techniques, via corrections and reformulations, to compensate for these systems; but the pairwise techniques discussed here require no modifications, making them natural tools to tackle these problems. Additionally, this transferability gives them ben-

efits over other pairwise methods, such as reaction field, because estimations of physical properties (e.g., the dielectric constant) are unnecessary.

If a researcher is using Monte Carlo simulations of large chemical systems containing point charges, most structural features will be accurately captured using the undamped SF method or the SP method with an electrostatic damping of  $0.2 \text{ \AA}^{-1}$ . These methods would also be appropriate for molecular dynamics simulations where the data of interest are either structural or short-time dynamical quantities. For long-time dynamics and collective motions, the safest pairwise method we have evaluated is the SF method with an electrostatic damping between  $0.2$  and  $0.25 \text{ \AA}^{-1}$ .

We are not suggesting that there is any flaw with the Ewald sum; in fact, it is the standard by which these simple pairwise sums have been judged. However, these results do suggest that in the typical simulations performed today, the Ewald summation may no longer be required to obtain the level of accuracy most researchers have come to expect.

#### ACKNOWLEDGMENTS

Support for this project was provided by the National Science Foundation under Grant No. CHE-0134881. The authors would like to thank Steve Corcelli and Ed Maginn for helpful discussions and comments.

- <sup>1</sup>B. Roux and T. Simonson, *Biophys. Chem.* **78**, 1 (1999).
- <sup>2</sup>C. Sagui and T. A. Darden, *Annu. Rev. Biophys. Biomol. Struct.* **28**, 155 (1999).
- <sup>3</sup>D. J. Tobias, *Curr. Opin. Struct. Biol.* **11**, 253 (2001).
- <sup>4</sup>M. Born, *Z. Phys.* **1**, 45 (1920).
- <sup>5</sup>A. Grossfield, J. Sachs, and T. B. Woolf, *Proteins* **41**, 211 (2000).
- <sup>6</sup>P. P. Ewald, *Ann. Phys. (Leipzig)* **64**, 253 (1921).
- <sup>7</sup>P. J. Steinbach and B. R. Brooks, *J. Comput. Chem.* **15**, 667 (1994).
- <sup>8</sup>L. Onsager, *J. Am. Chem. Soc.* **58**, 1486 (1936).
- <sup>9</sup>V. Rokhlin, *J. Comput. Phys.* **60**, 187 (1985).
- <sup>10</sup>D. Wolf, P. Koblinski, S. R. Phillpot, and J. Eggebrecht, *J. Chem. Phys.* **110**, 8255 (1999).
- <sup>11</sup>U. Essmann and M. L. Berkowitz, *Biophys. J.* **76**, 2081 (1999).
- <sup>12</sup>S. W. de Leeuw, J. W. Perram, and E. R. Smith, *Proc. R. Soc. London, Ser. A* **373**, 27 (1980).
- <sup>13</sup>M. P. Allen and D. J. Tildesley, *Computer Simulations of Liquids* (Oxford University Press, New York, 1987).
- <sup>14</sup>S. G. Brush, H. L. Sahlin, and E. Teller, *J. Chem. Phys.* **45**, 2102 (1966).
- <sup>15</sup>L. V. Woodcock and K. Singer, *Trans. Faraday Soc.* **67**, 12 (1971).
- <sup>16</sup>E. R. Smith, *Proc. R. Soc. London, Ser. A* **375**, 475 (1981).
- <sup>17</sup>N. Karasawa and W. A. Goddard III, *J. Phys. Chem.* **93**, 7320 (1989).
- <sup>18</sup>J. Kolafa and J. W. Perram, *Mol. Simul.* **9**, 351 (1992).
- <sup>19</sup>J. W. Perram, H. G. Petersen, and S. W. de Leeuw, *Mol. Phys.* **65**, 875 (1988).
- <sup>20</sup>R. W. Hockney and J. W. Eastwood, *Computer Simulation Using Particles* (McGraw-Hill, New York, 1981).
- <sup>21</sup>J. Shimada, H. Kaneko, and T. Takada, *J. Comput. Chem.* **14**, 867 (1993).
- <sup>22</sup>B. A. Luty, M. E. Davis, I. G. Tironi, and W. F. van Gunsteren, *Mol. Simul.* **14**, 11 (1994).
- <sup>23</sup>B. A. Luty, I. G. Tironi, and W. F. van Gunsteren, *J. Chem. Phys.* **103**, 3014 (1995).
- <sup>24</sup>T. Darden, D. York, and L. Pedersen, *J. Chem. Phys.* **98**, 10089 (1993).
- <sup>25</sup>U. Essmann, L. Perera, M. L. Berkowitz, T. Darden, H. Lee, and L. G. Pedersen, *J. Chem. Phys.* **103**, 8577 (1995).
- <sup>26</sup>D. E. Parry, *Surf. Sci.* **49**, 433 (1975).
- <sup>27</sup>D. E. Parry, *Surf. Sci.* **54**, 195 (1976).
- <sup>28</sup>D. M. Heyes, M. Barber, and J. H. R. Clarke, *J. Exp. Zool.* **73**, 1485 (1977).
- <sup>29</sup>S. W. de Leeuw and J. W. Perram, *Mol. Phys.* **37**, 1313 (1979).
- <sup>30</sup>Y.-J. Rhee, J. W. Halley, J. Hautman, and A. Rahman, *Phys. Rev. B* **40**,

- 36 (1989).
- <sup>31</sup>E. Spohr, J. Chem. Phys. **107**, 6342 (1997).
- <sup>32</sup>I.-C. Yeh and M. L. Berkowitz, J. Chem. Phys. **111**, 3155 (1999).
- <sup>33</sup>M. Kawata and M. Mikami, Chem. Phys. Lett. **340**, 157 (2001).
- <sup>34</sup>A. Arnold, J. de Joannis, and C. Holm, J. Chem. Phys. **117**, 2496 (2002).
- <sup>35</sup>J. de Joannis, A. Arnold, and C. Holm, J. Chem. Phys. **117**, 2503 (2002).
- <sup>36</sup>A. Bródka, Chem. Phys. Lett. **400**, 62 (2004).
- <sup>37</sup>J. E. Roberts and J. Schnitker, J. Chem. Phys. **101**, 5024 (1994).
- <sup>38</sup>J. E. Roberts and J. Schnitker, J. Phys. Chem. **99**, 1322 (1995).
- <sup>39</sup>B. A. Luty and W. F. van Gunsteren, J. Phys. Chem. **100**, 2581 (1996).
- <sup>40</sup>P. H. Hünenberger and J. A. McCammon, J. Chem. Phys. **110**, 1856 (1999).
- <sup>41</sup>P. H. Hünenberger and J. A. McCammon, Biophys. Chem. **78**, 69 (1999).
- <sup>42</sup>W. Weber, P. H. Hünenberger, and J. A. McCammon, J. Phys. Chem. B **104**, 3668 (2000).
- <sup>43</sup>D. Zahn, B. Schilling, and S. M. Kast, J. Phys. Chem. B **106**, 10725 (2002).
- <sup>44</sup>R. E. Jones and D. H. Templeton, J. Chem. Phys. **25**, 1062 (1956).
- <sup>45</sup>D. M. Heyes, J. Chem. Phys. **74**, 1924 (1981).
- <sup>46</sup>A. Rahman and F. H. Stillinger, J. Chem. Phys. **55**, 3336 (1971).
- <sup>47</sup>D. J. Adams, E. M. Adams, and G. J. Hills, Mol. Phys. **38**, 387 (1979).
- <sup>48</sup>T. A. Andrea, W. C. Swope, and H. C. Andersen, J. Chem. Phys. **79**, 4576 (1983).
- <sup>49</sup>J. A. Barker and R. O. Watts, Mol. Phys. **26**, 789 (1973).
- <sup>50</sup>N. Metropolis, A. W. Rosenbluth, M. N. Rosenbluth, A. H. Teller, and E. Teller, J. Chem. Phys. **21**, 1087 (1953).
- <sup>51</sup>See EPAPS Document No. E-JCPSA6-124-515622 for a comparative analyses of the pairwise cutoff method performance for each of the seven model systems studied. This document can be reached via a direct link in the online article's HTML reference section or via the EPAPS homepage (<http://www.aip.org/pubservs/epaps.html>).
- <sup>52</sup>H. J. C. Berendsen, J. R. Grigera, and T. P. Straatsma, J. Phys. Chem. **91**, 6269 (1987).
- <sup>53</sup>M. A. Meineke, C. F. Vardeman II, T. Lin, C. J. Fennell, and J. D. Gezelter, J. Comput. Chem. **26**, 252 (2005).
- <sup>54</sup>J. W. Ponder and F. M. Richards, J. Comput. Chem. **8**, 1016 (1987).
- <sup>55</sup>A. R. Leach, *Molecular Modeling: Principles and Applications*, 2nd ed. (Pearson Education Limited, Harlow, England, 2001).
- <sup>56</sup>S. M. Kast, K. F. Schmidt, and B. Schilling, Chem. Phys. Lett. **367**, 398 (2003).